Preparation and Characterization of Cu(II)- and Pt(II)-Thiourea Complexes and Adsorption of Pt(II) Complex on Local Bentonite

Ahmed Mohammed Sulaiman[1*] and Abdulaziz Khaled Awwad[2]

[1]*Department of Chemistry, College of Education, Al-Iraqia University, Al-Adhamiya, Baghdad 10053, Iraq*

[2]*General Directorate of Karkh III Education, Ministry of Education, Al-Kadhimiya, Baghdad 10006, Iraq*

** **Corresponding author:***

tel: +964-7500723382
email:
ahmed.m.sulaiman@aliraqia.edu.iq

Received: January 10, 2025
Accepted: March 31, 2025

DOI: 10.22146/ijc.103680

Abstract: *This study investigates the stability and adsorption behavior of inorganic complexes formed from the reaction of 2-aminopyridine with phenyl isothiocyanate to produce thiourea derivatives, which were further reacted with copper salts and platinum phosphine. The complexes were characterized using UV-vis and FTIR spectroscopies, revealing a 2:1 (ligand-to-metal) ratio and high stability. The effect of temperature on the stability showed a slight increase in absorption values with rising temperature. Stability constants and thermodynamic functions confirmed the complexes' stability at room temperature. Additionally, the adsorption of the platinum complex (AL2) onto bentonite clay was studied. Before and after adsorption, the bentonite surface was analyzed using UV-vis, FTIR, AFM, and SEM techniques. Adsorption isotherms followed Freundlich model, and adsorption kinetics followed first-order reaction model. The study aims to prepare and characterize copper-thiourea and platinum-phosphine complexes, calculate their stability constants, and explore the adsorption behavior of AL2 on bentonite. The results highlight the high stability of the complexes and the successful modeling of AL2 adsorption, suggesting their potential applications in catalysis and environmental remediation.*

Keywords: *thermodynamic; kinetics; adsorption; metal complexes; thiourea*

■ INTRODUCTION

The stability of metal complex is a crucial aspect of inorganic chemistry, drawing significant interest due to its implications for reaction kinetics, thermodynamic stability, and reaction mechanisms [1]. Thermodynamic stability focuses on the changes in free energy and entropy during reactions, offering insights into reaction direction [2]. The stability of a compound refers to its ability to exist under specific conditions without decomposition, maintaining its structural integrity over time [3]. Stability constants quantitatively describe the interaction strength between metal ions and ligands at the metal-ligand interface [4]. However, metal complex stability is context-dependent. A compound may remain stable under certain conditions but decompose when exposed to different reagents or environments [5]. The stability of coordination complexes can be further explained through thermodynamic stability, which reflects the overall energy changes during complex formation, and kinetic stability, which describes the reaction rate and resistance to ligand exchange [6].

Adsorption is a widely used method for removing metals from aqueous solutions, offering an effective and economical alternative to chemical precipitation, membrane separation, ion exchange, liquid-liquid extraction, and electrodialysis [7]. Traditional adsorbents, such as activated carbon, silica, and alumina, are effective but costly, driving research towards using natural, abundant, low-cost alternatives such as bentonite clay [8]. These natural adsorbents have shown considerable efficiency in extracting metals and organic pollutants, making them promising candidates for environmental remediation [9]. Studies have shown that the adsorption of metal complexes onto various substrates plays a key role in wastewater treatment and material recovery, highlighting the importance of optimizing adsorption

conditions and understanding surface interactions [10]. To measure metal concentrations in aqueous solutions, several analytical methods are employed, including flame atomic absorption spectrometry (FAAS), graphite furnace atomic absorption spectrometry (GFAAS), plasma atomic emission spectrometry, atomic fluorescence spectrometry (AFS), voltammetric methods, and UV-vis spectroscopy, the latter being applicable when metal ions form colored complexes [11-12].

Recent studies have also explored novel spectroscopic and electrochemical techniques to enhance the sensitivity and accuracy of metal ion detection, broadening the scope of analytical applications in coordination chemistry [13]. Building on these foundations, this study focuses on the preparation and characterization of Cu(II) and Pt(II) thiourea complexes and the adsorption behavior of the Pt(II) complex (AL2) onto local bentonite clay. The research explores the stability of these metal complexes by calculating their stability constants and thermodynamic properties while also investigating the adsorption isotherms and kinetics of AL2. By integrating complex stability studies with adsorption techniques, this work aims to comprehensively understand metal-ligand interactions and their potential applications in catalysis and environmental clean-up strategies.

■ EXPERIMENTAL SECTION

Materials

The materials used in this study were K_2PtCl_4 (98%, Chinese source), $C_{26}H_{24}P_2$ (97%, Chinese source), $C_5H_5N_2Cl$ (95.8%, Sigma Aldrich), $CuCl_2{\cdot}2H_2O$ (98.5%, BDH-UK), C_2H_5OH (99%, Scharlau), C_6H_6 (99.5%, SCR), CH_2Cl_2 (99.9%, Bio SoLVE), C_4H_8O (98%, Sigma Aldrich), and HCl (37% diluted, Sigma Aldrich), without additional purification.

Instrumentation

A variety of advanced instruments and techniques were employed in this study to ensure precise measurements and characterizations. UV-vis spectrophotometer (Shimadzu UV-Visible-1800, Japan, and Thermo Fisher Scientific, USA) was used to measure absorbance changes across wavelengths (190–1100 nm) using quartz cells with DMSO as the solvent. Infrared (IR) spectra of ligands and their metal complexes were recorded via FTIR spectrophotometry (Shimadzu-8400S, Japan) at the University of Tikrit. A pH meter (Jenway-3310, U.K.) was utilized to monitor pH variations. The adsorption process involving bentonite clay was analyzed using a centrifuge (Hettich zentrifugen 6000 rpm EBA 20, Germany) at the Iraqi University. Additionally, atomic force microscopy (AFM) (SPM AA3000 Angstrom Advanced Inc., USA) at the University of Baghdad and scanning electron microscopy (SEM) (Nova NanoSEM 450) at the University of Basra provided surface morphology insights, ensuring a comprehensive study of the complexes and their adsorption behavior.

Procedure

Preparation of the first ligand (L1)

Phenyl isothiocyanate (0.53 g, 3.89 mmol) was added to a solution of 5-chloro-2-aminopyridine (0.51 g, 3.89 mmol) in 40 mL of tetrahydrofuran (THF). The solution was left to stir and rise for 4 h at 35–45 °C. The solution was filtered and it was cooled to obtain the precipitate, dried, and recrystallized twice with absolute ethanol to obtain a pure substance, after which it was filtered and washed with ethanol. The result is a white cottony precipitate with a weight of 0.845 g and a percentage of 82%. The melting point is 191–194 °C, and the FTIR analysis is carried out on the synthesized ligand [14].

Preparation of cis-*[$PtCl_2(DMSO)_2$]*

$K_2[PtCl_4]$ (0.500 g, 1.204 mmol) salt was dissolved in 5 mL of distilled water, and then 0.170 mL of dimethyl sulfoxide (DMSO) was added to the stirred solution. The mixture was left for 1 d until pale yellow needle crystals were obtained. The crystals were filtered, washed with diethyl ether, and dried under low pressure to yield 0.389 g (77%).

Preparation of [$PtCl_2$(dppe)] (X1)

To a stirred volume 10 mL of dichloromethane solvent in which of *cis*-[$PtCl_2(DMSO)_2$] (0.150 g, 0.356 mmol) is dissolved, 2,1-di(diphenylphosphine)ethane (DPPE) (141 g, 0.356 mmol) previously dissolved in 10 mL of the same solvent as the clear solution changed color to white. The

mixture was stirred for 2 h and the pale-yellow solution was transferred to a beaker and left at room temperature for slow evaporation to give white crystals weighing 0.23 g with 95% yield and a melting point of 279–282 °C.

Preparation of copper complex (AL1)

The complex was prepared with a molar ratio of 2:1 (metal:ligand), where 0.22 g (9.48×10^{-5} mol) of $CuCl_2 \cdot 2H_2O$ was dissolved in 15 mL absolute ethyl alcohol, then 0.05 g (1.89×10^{-4} mol) of L1 in 10 mL of the same solvent. After dissolving the ligand, it was gradually added to the metal with continuous stirring. The color changed immediately from dark green to light green. The mixture was left to stir and rise for 4 h at 35–45 °C and left aside to cool. A light blue precipitate was obtained to be filtered and dried.

Preparation of platinum complex (AL2)

In a beaker glass, 0.05 g (7.5×10^{-5} mol) of X1 was dissolved in 10 mL of dichloromethane. Then, a 0.017 g (7.5×10^{-5} mol) L1 dissolved in 10 mL of absolute ethanol containing 0.008 g (1.5×10^{-4} mmol) of KOH. The mixture was refluxed for 2 h, and a light-yellow color was observed when the desired precipitate appeared. The product was filtered and dried by a vacuum dryer, and the precipitate weighed 0.0465 g with a percentage of 80%.

Preparation of complexes in the form of solutions

After conducting the necessary test to discover the appropriate solvent for these complexes, DMSO is found to be the most suitable solvent for the measurements needed in this work. A reference solution of the previously prepared copper complex, from the reaction of thiourea-derived ligand with copper(II) chloride at a concentration of 1×10^{-2} mM was prepared by dissolving 0.295 g of the precipitate in 25 mL of DMSO, then completing the volume with the same solvent to the mark in a volumetric flask 50 mL. The rest of the series of concentrations of 0.001, 0.0001, 0.00001, 0.00001, and 0.000001 mM were prepared after making the required dilution of the reference solution. Also, the same process was done for the previously prepared platinum complex from the reaction of a thiourea derivative ligand with the platinum-phosphine complex at a concentration of 1×10^{-2} M was carried out by dissolving 0.292 g of the precipitate in DMSO.

Adsorbate and adsorbent

The adsorbent used in this research was bentonite clay obtained from public markets. The chemical analysis of the clay is listed in Table 1.

Preparation of bentonite clay

The bentonite clay used in this study was obtained from one of the perfume shops in popular markets. The clay was washed in powder form with an appropriate amount of distilled water to about 16 times to remove water-soluble substances and foreign substances. Then, the clay was dried in an electric oven at 150 °C for 3 h. The dried bentonite clay is ground to fine flour. The ground powder was sieved using sieves of different sizes to obtain the desired size of 150, 200, and 250 μm.

Adsorption experiment

Equilibrium time of adsorption systems. The equilibrium time between AL2 and the bentonite surface was determined for the adsorption process to reach equilibrium. All conditions were stabilized from the concentration of 80.30 mg/L, the weight of the adsorbent was 0.085 g, the size of the adsorbent was 150 μm, and the volume of solution 10 mL was used. The volumetric flasks were placed in a shaking water bath at 25 °C. Samples were withdrawn from the water bath at different time intervals ranging from 5–120 min, and their absorbance was measured after separation in a centrifuge at 6000 rpm and filtration and by following the change of absorbance values with time and then determining the equilibrium time of the AL2 complex with the adsorbent surfaces.

Effect of adsorbent weight. The weight of the adsorbent bentonite clay that gives the highest adsorption was determined by taking different weights

Table 1. Chemical analysis of bentonite clay components

Na_2O	Fe_2O_3	SiO_2	Al_2O_3	CaO	SO_3	MgO	L.O.I*	Total
0.65	4.88	54.66	14.65	4.77	1.20	6.00	12.56	99.37

* L.O.I = Loss on ignition

of the adsorbent ranging from 0.025–0.16 g and the size of min. First, an adsorbent with a particle size of 150 µm was placed in contact with 80.30 mg/L of AL2, then all were placed in a shaking water bath at a constant temperature of 25 °C. The samples were withdrawn from the water bath, and their absorbance was measured after the separation process in a centrifuge at 6000 rpm filtration speed.

Effect of pH. The adsorption of the AL2 complex on the bentonite surface was studied in different acidic media using dilute solutions of 0.1 M HCl and 0.1 M NaOH at a constant AL2 concentration of 80.30 mg/L and adsorbent weight of 0. 085 g for the bentonite clay and the size of the fines of 150 µm. All were placed in a shaking water bath for 45 min at 25 °C, then the samples were withdrawn from the water bath, the adsorbent surface was separated, and the absorbance was measured using a UV-vis spectrometer.

Effect of particle size. To study the effect of adsorbent particle size on adsorption capacity, three different adsorbent particle sizes, i.e., 100, 150, and 200 µm were used. These experiments were conducted using a constant concentration of 80.30 mg/L of AL2 solution and adsorbent weight 0.085 g of bentonite clay. Then the samples were placed in a shaking water bath for 45 min at a temperature of 25 °C. The samples were withdrawn, and their absorbance was measured after the separation process in the centrifuge at 6000 rpm for the filtration process.

■ RESULTS AND DISCUSSION

Characterization of Prepared Compounds

The compounds needed for this study were prepared according to the designed method, and the compositions of the compounds, as shown in Scheme 1, were proposed after their UV-vis and FTIR spectroscopic characterization.

UV-vis spectra

The spectrum of L1 gave two absorption bands (Fig. S1), where the first with greater intensity and lower wavelength is attributable to transitions of the π-π*, which is caused by C=S and C=C aromatic bonds. It is noticeable that it appeared in the range of 202–282 nm and is shifted at longer values compared to π-π* for the isothiocyanobenzene compound, which may be explained by the increased length of the coupled system of the thiourea derivatives.

The second band with lower intensity and larger wavelength appeared in the range of 218–288 nm, which is attributed to n-π* type electronic transitions caused by unshared electron pairs on the oxygen, nitrogen, and sulfur atoms, and these values were observed to be redshifted.

The electronic spectrum of the Cu(II) complex showed a broad, medium-intensity absorption peak in the range of 631–665 nm belonging to the electronic transition of $A_{1g} \rightarrow {}^1B_{1g}{}^1$ and is consistent with the results

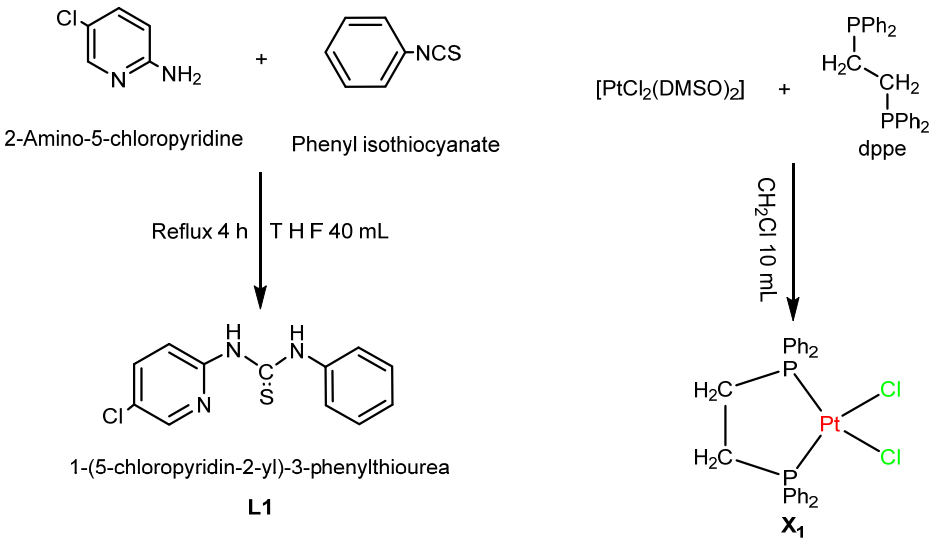

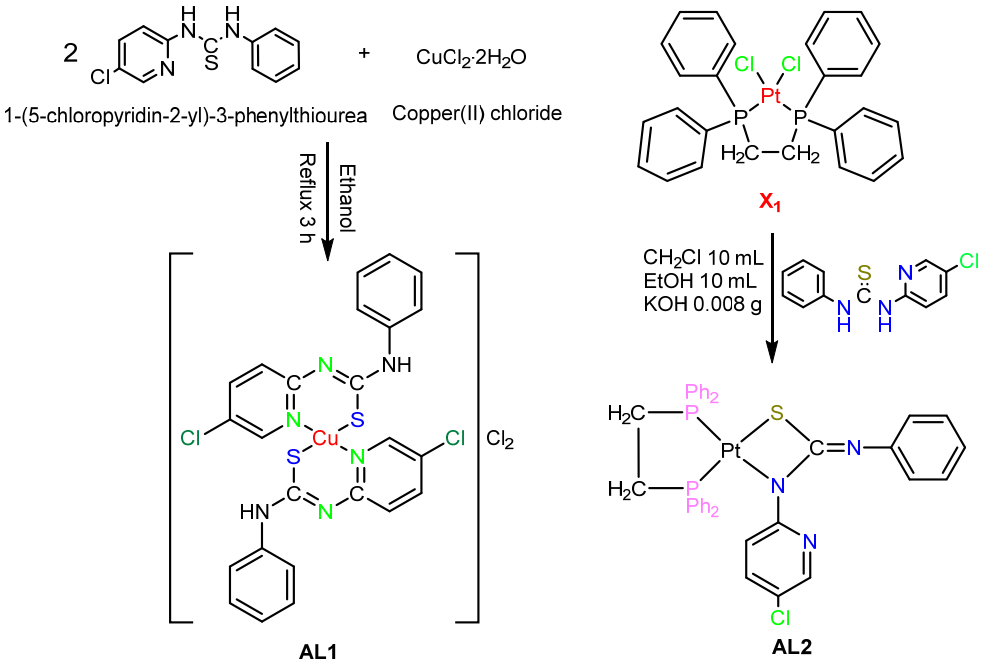

Scheme 1. Proposed structures of compounds

Table 2. Electronic spectroscopy measurements of ligand and complexes

Complexes	λ (nm)	ν (cm^{-1})	Transitions
L1	246	40650.4	π–π*
	273	36630.0	n–π*
AL1	621	16103.0	$^2E_g \rightarrow {}^2T_{2g}$
AL2	567	17636.6	$^1A_{1g} \rightarrow {}^1B_{1g}$

for planar square-planar tetrahedral copper [15]. The UV-vis absorption spectrum of this complex showed a broad peak between 234–275 nm representing the ligand-centered domain, and the visible region showed a single peak at 567 nm belonging to the $^1A_{1g} \rightarrow {}^1B_{1g}$ transition. As shown in Fig. S1, these solutions showed a color-spectral change accompanied by a red shift of the peaks in the range of 200–400 nm. Table 2 shows the most important electronic transitions for ligand and their metal complexes under study.

FTIR spectra

The reaction and product formation were confirmed using FTIR spectroscopy. The spectrum showed the expected absorption bands, as shown in Table 3. The prepared complexes were characterized and compared with the spectrum of free ligands, as some bands displaced and some disappeared with the appearance of other new bands, indicating the formation of ligand on the one hand and the coordination between it and the metals on the other hand, as shown in Fig. S2.

The Effect of Temperature on the Stability of Complexes

This study used spectroscopic methods to calculate the stability constants of the complexes in solution. Before carrying out the measurements, the ideal experimental conditions such as concentration, pH, and time were optimized. The resulting solutions exhibited

Table 3. Characteristic packets of ligands and their complexes

Complexes	N–H	=C–H aromatic	C–H aliphatic	C=C	C=N	C=S	Others
L1	3302	3032	-	1531	1600	630	C–Cl, 819
AL1	3417	3026	-	1560	1595	831	Cu–S, 459
							Cu–N, 536
AL2	-	3051	2955	1554	1635	827	Pt–S, 488
							Pt–N, 532

clear and distinct colors, with absorption peaks appearing in the visible region of the spectrum. Stability constants were then determined at various temperatures ranging from 30-70 °C, using the optimal concentration. The calculations were based on Eq. (1) and (2);

$$\begin{matrix} m^{+n} + nL \rightleftharpoons ML_n \\ \alpha C \quad nC\alpha \quad (1-\alpha)C \end{matrix} \quad (1)$$

$$K = \frac{\left[ML^{+n}\right]}{\left[M^{+n}\right]\left[L\right]} \quad (2)$$

where the M = metal ion, L = ligand, n = molar ratio = 2, α = degree of dissociation, and C = molar concentration of the complex formed. K can be expressed as in Eq. (3) and (4);

$$K = \frac{(1-\alpha)C}{\alpha C \times 2\alpha C} \quad (3)$$

$$K = \frac{(1-\alpha)}{2\times\alpha^2 \times C} \quad (4)$$

α can be calculated from the following relationship in Eq. (5);

$$\alpha = \frac{A_m - A_s}{A_m} \quad (5)$$

A_m is the highest absorbance of the node, and A_s is the lowest absorbance of the complex. Table 4 shows the stability constants for the complexes.

The results of this study showed that the values of K increase gradually with the increase in temperature. This is coming from the fact that the rise in the latter leads to an increase in the degree of formation of these complexes and a decrease in the degree of their dissociation (α).

Calculation of Thermodynamic Functions

The thermodynamic functions calculated for the complexes prepared in this study are in a range of different temperatures, ranging from 303–343 K, as shown in Table 5. Fig. 1 shows a gradual increase in the values of the stability constants as the temperature increases. The increase in the values of the stability constants in this study with increasing temperature allows

Table 4. Stability constants for the complexes

Complex	T (K)	A_s	A_m	α	K	ln K
AL1	303	0.232	0.291	0.203	9702.20	11.48
	313	0.269	0.315	0.146	200319.01	12.20
	323	0.298	0.340	0.123	289840.70	12.56
	333	0.447	0.489	0.085	633218.00	13.36
	343	0.462	0.502	0.079	737862.50	13.51
AL2	303	0.342	0.559	0.388	2032.63	7.61
	313	0.358	0.571	0.373	2253.30	7.72
	323	0.374	0.581	0.356	2540.71	7.84
	333	0.399	0.605	0.340	2854.67	7.95
	343	0.415	0.613	0.323	3244.54	8.08

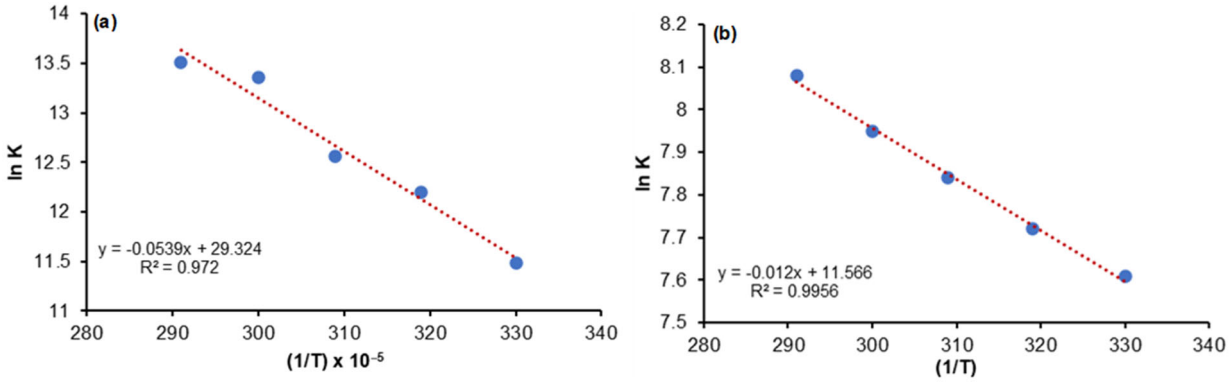

Fig 1. Graphs between ln k and 1/T for (a) AL1 and (b) AL2 complexes

Table 5. Values of thermodynamic functions for complexes at different temperatures

Complex	T (K)	$(1/T) \times 10^{-5}$	ln K	ΔG (kJ/mol)	ΔH (kJ/mol)	ΔS (J/mol)
	303	330	11.48	−28.92		95.44
	313	319	12.20	−31.74		101.40
AL1	323	309	12.56	−33.73	4.48×10^{-4}	104.42
	333	300	13.36	−36.98		111.00
	343	291	13.51	−38.52		112.00
	303	330	7.61	−19.17		63.26
	313	319	7.72	−20.09		64.18
AL2	323	309	7.84	−21.05	1×10^{-4}	65.17
	333	300	7.95	−22.01		66.09
	343	291	8.08	−23.04		67.17

us to study this reaction from the thermodynamic point of view, i.e., extracting the thermodynamic variables from the van't Hoff integral equation as shown in Eq. (6);

$$\ln K = \frac{-\Delta H}{RT} + C \quad (6)$$

where the K = stability constant, R = gas constant 8.314 J/mol K, and T = absolute temperature (K). The Gibbs free energy is calculated using the Eq. (7);

$$\Delta G = -RT \ln K \quad (7)$$

The change in entropy ΔS can be calculated from the relationship between ΔG, ΔH, and ΔS, which is represented by Eq. (8) and (9).

$$\Delta G = \Delta H - T\Delta S \quad (8)$$

$$\Delta S = (\Delta H - \Delta G)/T \quad (9)$$

Positive values of the enthalpies of the reaction indicate that the reaction is endothermic. Also, the coordination process appears to be spontaneous due to the negative free energy values. As it is known that entropy is a measure of randomness, theoretically, the entropy is positive because high values of entropy push the reaction to the right (i.e., towards the products and complex formation) [16-17].

Adsorption Study

FTIR spectra

The FTIR analysis of the bentonite clay components was carried out. Fig. S2 shows bands at 3614 and 872 cm^{-1} due to Al–OH stretching and Al–OH bending, respectively. Peaks showed at 3418 and 1636 cm^{-1} due to O–H stretching and bending, respectively. The strong band at 1022 cm^{-1} is due to Si–O stretching. We noted that the band of quartz, the mineral associated with bentonite, was weak at 663.51 cm^{-1}.

AFM analysis

AFM image of bentonite before adsorption shows that the size distribution of the bentonite clay is between 30–115 nm, and this size distribution represents the growth limit of the bentonite clay microcrystals and the maximum height reached by these particles at 22.14 nm. We also observe in Fig. 2, the AFM image of the bentonite particles after adsorption, a decrease in the contrast between the particles after the adsorption process, and on the other hand, the size distribution range of the bentonite particles has increased from 60–230 nm, and the maximum height of these particles reaches 18.33 nm, which is evidence that there is an association between the complex and the surface of the bentonite clay.

SEM analysis

SEM shows the crystal structure, surface texture, and porosity of the adsorbed material. The SEM micrograph of the untreated bentonite clay sample (before adsorption) indicates a highly cohesive material, as shown in Fig. 3. The micrograph magnified at 20000× confirms that the material forms micron-sized agglomerates like agglomerated sheets containing some pores. After the adsorption process, the SEM micrograph at 50000× magnification showed that the exterior of the clay was covered with a thin layer of adsorbent, which appeared on a number of similar agglomerates, as in Fig. 3.

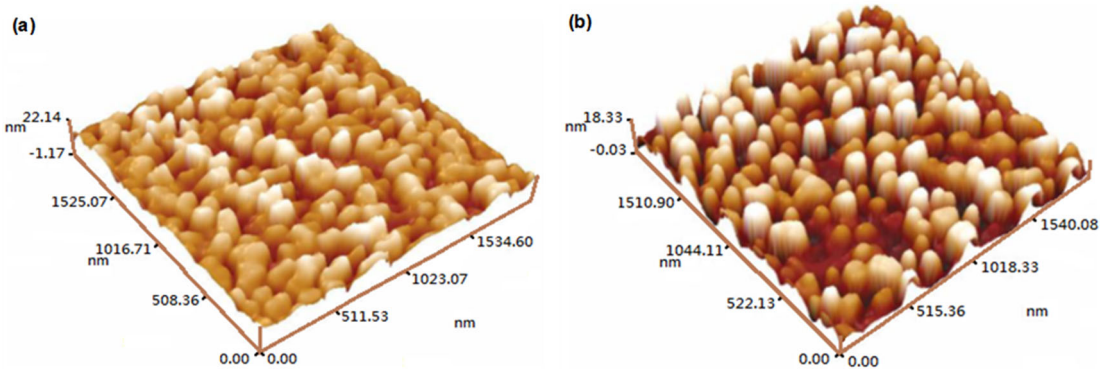

Fig 2. AFM of the bentonite surface (a) before adsorption and (b) after adsorption

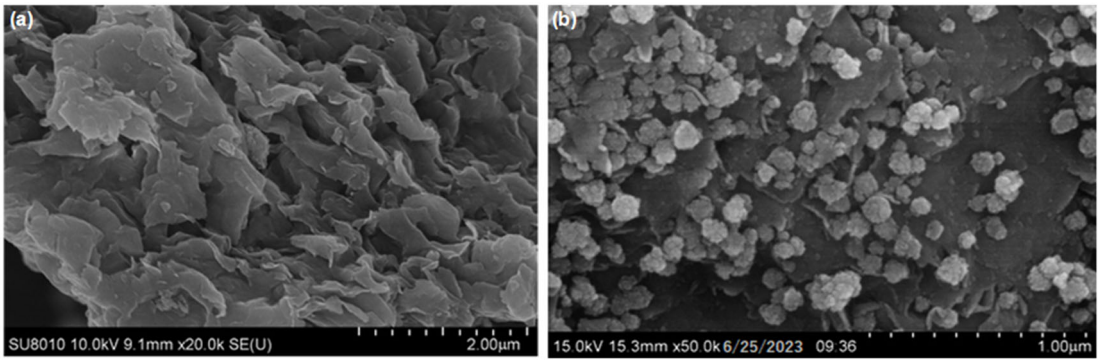

Fig 3. SEM of the bentonite surface (a) before adsorption and (b) after adsorption

Effect of adsorbent weight

The effect of the weight of the adsorbent on the adsorption process was studied. This study was carried out using a concentration of 80.30 mg/L of the compound solution with different weights ranging from 0.025–0.16 g of bentonite clay adsorbed at a temperature of 25 °C and a size of the adsorbent particles of 150 µm. Table 6 and Fig. 4 show the effect of changing the weight of the adsorbent with the clay removal percentage.

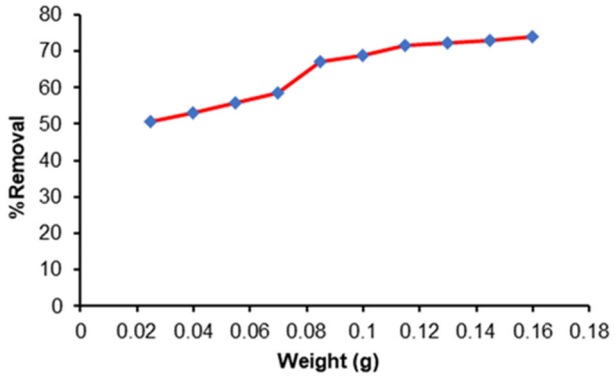

Fig 4. Effect of changing the weight of the adsorbent with the removal ratio for bentonite clay

Table 6. Effect of changing the adsorbent weight with the removal ratio for bentonite clay

Adsorbent weight (g)	Bentonite	
	C_e (mg/L)	%Removal
0.025	39.545	50.75
0.040	37.626	53.14
0.055	35.519	55.76
0.070	33.213	58.63
0.085	26.334	67.20
0.100	24.911	68.97
0.115	22.731	71.69
0.130	22.236	72.31
0.145	21.645	73.04
0.160	21.011	73.83

The effect of increasing the adsorbent amount on the adsorption process is stratified when the weight of the adsorbent used is less than 0.085 g under the conditions of the mentioned experiment, and then there is a significant increase in the amount of adsorbent after this weight and no significant change in the removal values is observed after that [18].

Table 7. Change of concentration values at equilibrium with time on a bentonite surface

Adsorbent	C_0 (mg/L)	Time (min)	C_e (mg/L)	%Removal of the ions	Equilibrium time (min)
Bentonite	80.30	5	30,112	62.500	60
		15	30.954	61.452	
		30	32.660	59.327	
		45	35.371	55.951	
		60	32.453	59.585	
		75	29.979	60.666	
		90	29.859	60.815	
		120	28.771	62.170	

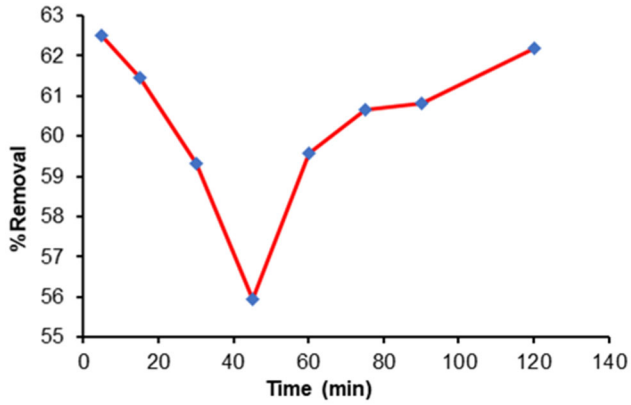

Fig 5. AL2 equilibrium time on a bentonite clay surface

Effect of contact time

The time required to reach equilibrium in the adsorption process of AL2 on the bentonite surface was studied for different time ranges (5–120 min) at a temperature of 25 °C and a constant concentration of 80.30 mg/L for AL2 using the size of the adsorbent fines 150 µm. A constant weight of clay 0.085 g was used, and the study results are shown in Table 7 and Fig. 5. The results show that the time required to reach equilibrium and the percentage removal of complex ions in the clay is 60 min. These values were adopted as equilibrium times for the adsorption systems.

It can be seen from the equilibrium time curves that the number of adsorbents decreases rapidly during the first few minutes of the process and then, at 60 min reaches an almost stable value [18].

Effect of pH

The adsorption of AL2 on the surface of bentonite clay with different pH, was studied at the constant concentration (80.30 mg/L), temperature (25 °C), particle size (150 µm), and removal time (60 min) as shown in Table 8 and Fig. 6. Experimental results demonstrated an inverse correlation between pH elevation and removal efficiency. Maximum adsorption efficiency (70.39%) was observed at acidic pH (1.66), with a gradual decline in performance as pH increased, stabilizing near 55% under alkaline conditions (pH > 7). Concurrently, the equilibrium concentration (C_e) increased from 23.777 to 35.671 mg/L within the tested

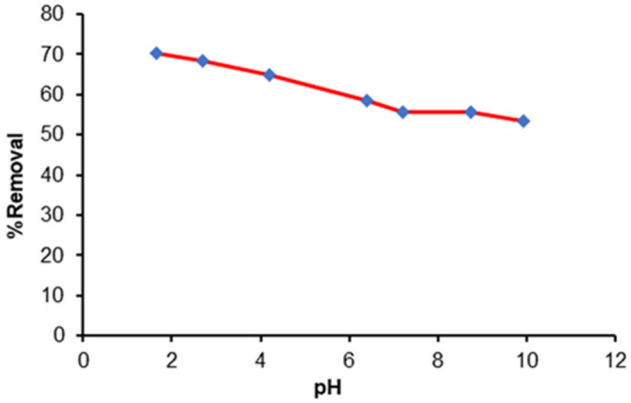

Fig 6. Effect of pH on the adsorption of AL2 on the bentonite surface

Table 8. Effect of changing pH with removal ratio for bentonite clay

Adsorbent	pH	C_e (mg/L)	%Removal
Bentonite	1.66	23.777	70.39
	2.70	25.518	68.22
	4.20	28.221	64.85
	6.40	33.437	58.36
	7.20	35.671	55.57
	8.75	35.573	55.74
	9.91	35.014	53.39

pH range. This phenomenon is attributed to electrostatic interactions between the permanently negatively charged bentonite surface, a consequence of isomorphous substitution within its aluminosilicate lattice, and the ionization state of the AL2 complex. Under acidic conditions (pH < 7), proton (H^+) saturation neutralizes the clay's surface charge, minimizing electrostatic repulsion and promoting the adsorption of cationic or neutral AL2 species. Conversely, elevated pH enhances surface negativity via hydroxyl (OH) group deprotonation, inducing repulsive forces against anionic AL2 forms. Furthermore, hydroxyl ions (OH^-) in alkaline media may compete for adsorption sites or form complexes with AL2, further reducing removal efficacy. The stabilization of R% beyond pH 7 likely reflects the equilibrium between electrostatic repulsion and secondary adsorption mechanisms, such as van der Waals interactions or partial site saturation. These findings underscore bentonite's potential as a cost-effective adsorbent for cationic contaminants in acidic environments, though its utility diminishes under alkaline conditions [19].

Effect of particle size

The effect of adsorbent particle size on the adsorption process using a concentration (80.30 mg/L) of AL2 solution, bentonite adsorbent weight (0.085 g) with different adsorbent particle size. Table 9 and Fig. 7 show the effect of adsorbent particle size on the amount of adsorption on the clay surface. The relationship between the amount of adsorption and the particle size of the adsorbent is inverse, as the amount of adsorption decreases as the size of the fines increases. This is because increasing the size of the fines reduces the surface area, which reduces the removal rate [20].

The Adsorption Isotherms of AL2 Complex

The adsorption of AL2 from its solution on the surface of bentonite clay was studied using two adsorption models: Langmuir and Freundlich [21]. Langmuir adsorption is modeled in the following Eq. (10) [22];

$$\frac{1}{q_e} = \frac{1}{q_m} + \frac{1}{b \cdot q_m \cdot C_e} \quad (10)$$

Table 9. Effect of adsorbent particle size on the amount of adsorption on the surface of bentonite clay

Particle size (μm)	Bentonite	
	C_e (mg/L)	q_e (mg/g)
150	37.513	5.033
200	43.917	4.280
250	45.936	4.042

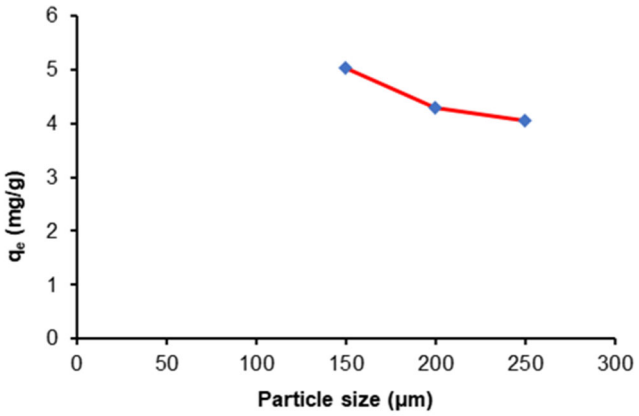

Fig 7. Effect of adsorbent particle size on the adsorption of AL2 complex on the surface of bentonite clay

where the C_e and q_e are the concentration at equilibrium (mg/L) and the quantity of AL2 adsorbed onto bentonite clay (mg/g), respectively. q_m (mg/g) is the maximum adsorption capacity. Then, b represents the Langmuir constant, which is related to the adsorption energy or equilibrium constant. The Langmuir constants were extracted by plotting $(\frac{1}{q_e})$ against $(\frac{1}{C_e})$, where the intercept and slope are $(\frac{1}{b \cdot q_m})$ and $(\frac{1}{q_m})$.

The Langmuir isotherm equation was applied for the adsorption of the AL2 complex on the surface of bentonite clay at different temperatures, as shown in Fig. 8 and Table 10. The key feature of the Langmuir model is the calculation of the separation coefficient (R_L), which predicts the type of adsorption system, whether it is favored or not, which is calculated from the following Eq. (11).

$$R_L = \frac{1}{1 + b \cdot C_0} \quad (11)$$

In bentonite, the adsorption isotherms at the studied temperatures show a good fit to the Langmuir adsorption model with a small value of R_L less than one

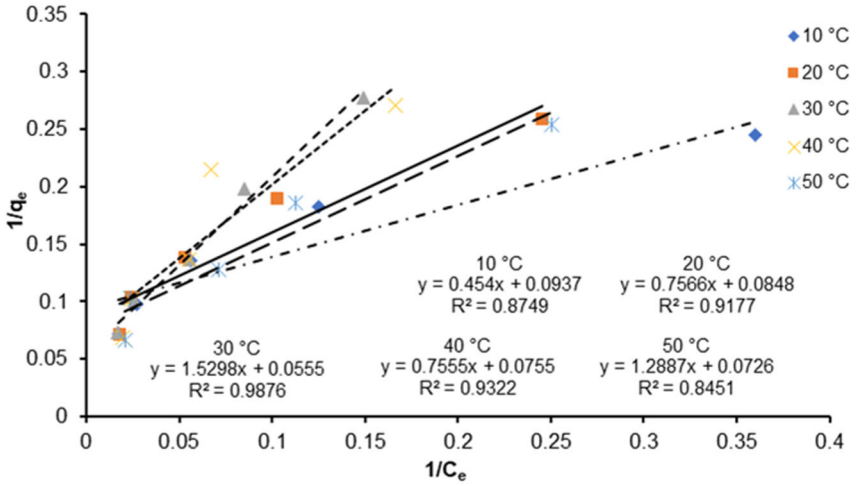

Fig 8. Langmuir isotherm for adsorption of the AL2 complex on the surface of bentonite clay

Table 10. Values of Langmuir constants and separation coefficient for the adsorption of AL2 on the surface of bentonite clay

Adsorbate	Temperature (K)	q_{max} (mg/g)	b	R_L
Clay	283	10.677	0.206	0.0570
	293	11.793	0.112	0.1000
	303	18.030	0.036	0.0007
	313	13.773	0.056	0.0009
	323	13.246	0.099	0.0009

and positive slope and intercept values for all isotherms, which means that they give realistic estimates of the adsorption process constant (b) and q_{max} value. From the q_{max} values obtained from Langmuir isotherm, we find that the value is greater at temperatures of 20 and 30 °C as a new adsorption layer is formed. Still, when the temperature increases, the value of q_{max} decreases because the process is thermalized, and the number of adsorbents decreases [23-24]. The obtained R_L values show that the adsorption process is preferred because it is less than the correct one [25].

The second model is the Freundlich model, which is used to represent the adsorption of a heterogeneous system [26]. The Freundlich model is summarized in the following Eq. (12);

$$\log q_e = \log K_F + \frac{1}{n}\log C_e \quad (12)$$

where K_F (slope, mg/g) represented adsorption capacity and n (intercept, unit less) represented adsorption intensity. The Freundlich constant (K_F, n) was calculated by drawing log q_e against log C_e, as shown in Tables 11 and 12. The plot of log q_e vs. log C_e was shown in Fig. 9.

Table 12. Values of experimental Freundlich constants and correlation coefficient values for the adsorption of AL2 on the surface of bentonite clay

Adsorbate	T (K)	K_F (mg/g)	n	R^2
Clay	283	2.542	2.532	0.9767
	293	1.795	2.066	0.9713
	303	1.251	1.716	0.9875
	313	1.102	1.613	0.9130
	323	2.026	2.111	0.9213

Table 11. log C_e and log q_e values for the adsorption of complex AL2 on the surface of bentonite clay

Adsorbate	283 K		293 K		303 K		313 K		323 K	
	log C_e	log q_e	log C_e	log q_e	log C_e	log q_e	log C_e	log q_e	log C_e	log q_e
Bentonite	0.443	0.610	0.654	0.587	0.790	0.556	0.779	0.567	0.602	0.594
	0.902	0.738	0.988	0.722	1.070	0.702	1.174	0.668	0.949	0.729
	1.252	0.866	1.270	0.861	1.253	0.865	1.254	0.865	1.144	0.892
	1.562	1.011	1.615	0.986	1.592	0.997	1.605	0.991	1.620	0.984
	1.762	1.139	1.743	1.149	1.767	1.137	1.709	1.163	1.681	1.175

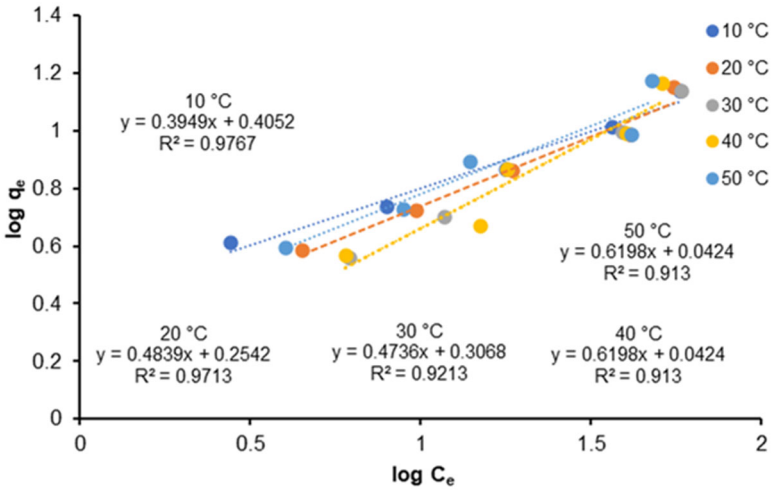

Fig 9. Isotherm Freundlich for adsorption of the AL2 complex on the surface of bentonite clay

When the previous data were represented by the Freundlich adsorption isotherm, as shown in Fig. 9, it was found that most of the isotherms show excellent compliance with the Freundlich isotherm but with very low values of adsorption capacities. This supports our previous discussion of the isotherms in that the growth of the amounts of adsorbent that took the L1 and S1 patterns at different temperatures did not reach the saturation of the surface, and this is due to the relatively low concentration of the adsorbent used in this study [27-28].

The n-values of adsorption intensity calculated by Freundlich isotherm indicate a state of rapid growth of the amount of material adsorbed on the surface [29]. The constant values show the degree of non-linearity between (n) solution concentration and adsorption. If $n = 1$ adsorption is linear, $n < 1$ adsorption is a chemical process, and $n > 1$ adsorption is a physical process. The values of n for the systems under study are greater than 1, indicating that adsorption is a physical process [30].

Kinetics Adsorption of AL2 Complex on the Surface of Bentonite Clay

The adsorption velocity rate constant was extracted from the Lagergren equation [31]. This method is based on the difference between the amount of adsorbent at equilibrium (q_e) and its amount at a given time (q_t) and is equivalent to the first-order equations in Eq. (13) [32];

$$\log(q_e - q_t) = \log q_e - \left(\frac{K_{ad}}{2.303}\right)t \qquad (13)$$

where $q_e = (C_0 - C_e)$ and its unit is mg/L, $q_t = (C_0 - C_t)$ and its unit mg/g, and K_{ad} adsorption rate constant.

The results are shown in Table 13. obtained according to Lagergren's equation, the slope of the plotted linear relationship between the values of log ($q_e - q_t$) versus time (t) was calculated from the results in Table 14, and Fig. 10 illustrates the plot. The value of K_{ad} was calculated as shown in Table 15.

Table 13. Time-varying effect of complex solution (AL2) at different concentrations

t	C_0 = 37.42 mg/L		C_0 = 54.54 mg/L		C_0 = 80.30 mg/L		C_0 = 123.72 mg/L		C_0 = 175.10 mg/L	
	C_t	C_e	C_t	C_e	C_t	C_e	C_t	C_e	C_t	C_e
15	5.153	3.932	10.733	9.937	13.564	12.543	36.012	35.046	51.695	50.828
30	3.892	2.953	10.574	9.937	13.338	12.543	35.778	35.046	51.523	50.828
45	3.686	2.953	10.453	9.937	13.074	12.543	35.595	35.046	51.408	50.828
60	3.473	2.954	10.325	9.937	13.018	12.543	35.551	35.046	51.261	50.828
75	3.395	2.953	10.213	9.937	12.904	12.543	35.392	35.046	51.160	50.828
90	3.282	2.953	10.158	9.937	12.842	12.543	35.324	35.046	51.092	50.828

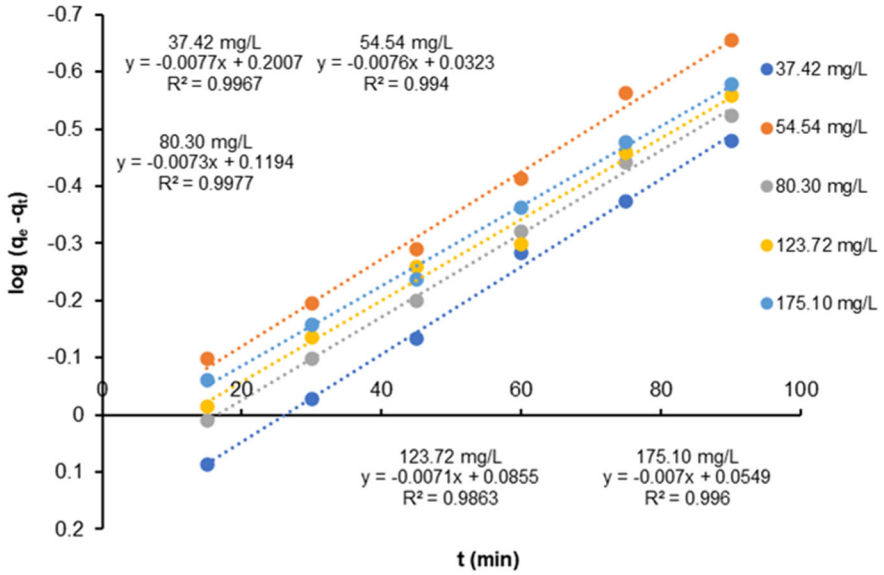

Fig 10. Lagergren lines for AL2 adsorption on a bentonite clay surface

Table 14. Effect of changing the initial concentration of complex solution (AL2) on its adsorption kinetics on the surface of bentonite clay

t (min)	C_0 = 37.42 mg/L				C_0 = 54.54 mg/L				C_0 = 80.30 mg/L			
	q_t	q_e	$(q_e - q_t)$	log $(q_e - q_t)$	q_t	q_e	$(q_e - q_t)$	log $(q_e - q_t)$	q_t	q_e	$(q_e - q_t)$	log $(q_e - q_t)$
15	32.265	33.487	1.222	0.087	43.805	44.602	0.797	−0.098	66.735	67.758	1.023	0.009
30	33.529	34.468	0.939	−0.027	43.964	44.602	0.638	−0.195	66.961	67.758	0.797	−0.098
45	33.735	34.468	0.733	−0.134	44.088	44.602	0.514	−0.289	67.227	67.758	0.531	−0.199
60	33.947	34.468	0.521	−0.283	44.216	44.602	0.386	−0.413	67.281	67.758	0.477	−0.321
75	34.026	34.468	0.422	−0.374	44.328	44.602	0.274	−0.562	67.397	67.758	0.361	−0.442
90	34.137	34.468	0.331	−0.480	44.381	44.602	0.221	−0.655	67.459	67.758	0.299	−0.524

t (min)	C_0 = 123.72 mg/L				C_0 = 175.10 mg/L			
	q_t	q_e	$(q_e - q_t)$	log $(q_e - q_t)$	q_t	q_e	$(q_e - q_t)$	log $(q_e - q_t)$
15	87.709	88.673	0.964	−0.015	123.405	124.272	0.867	−0.061
30	87.941	88.673	0.732	−0.135	123.577	124.272	0.695	−0.158
45	88.124	88.673	0.549	−0.260	123.692	124.272	0.580	−0.236
60	88.170	88.673	0.503	−0.298	123.839	124.272	0.433	−0.363
75	88.327	88.673	0.346	−0.460	123.940	124.272	0.332	−0.478
90	88.397	88.673	0.276	−0.559	124.008	124.272	0.264	−0.578

Table 15. K_{ad} values at different concentrations

C_0 (mg/L)	K_{ad}
37.42	0.017656333
54.54	0.017590533
80.30	0.016752680
123.72	0.016375427
175.10	0.016107840

The values of the adsorption constant were found in Table 15, which indicates that the reaction is proportional to the first-order literature according to the Lagergren equation.

■ CONCLUSION

In conclusion, this study successfully synthesized and characterized copper-thiourea and platinum-phosphine complexes, confirming a (2:1) ligand-to-metal ratio through UV-vis and FTIR spectroscopies. The stability constants and thermodynamic analysis demonstrated that the complexes are highly stable at

room temperature, with a slight increase in absorption values as temperature rises. The adsorption behavior of AL2 onto bentonite clay was thoroughly investigated, with adsorption isotherms aligning more closely with the Freundlich model than the Langmuir model. Kinetic studies revealed that the adsorption process is physical and follows apparent first-order reaction kinetics. The findings have significant implications for both catalysis and environmental remediation. The high stability of the synthesized complexes suggests their potential use as catalysts in various chemical processes. Additionally, the successful adsorption of AL2 onto bentonite indicates a promising approach for removing metal complexes from aqueous environments, contributing to wastewater treatment strategies. These results pave the way for further research into the practical applications of these inorganic complexes in industrial and environmental contexts.

■ ACKNOWLEDGMENTS

The authors thank the Al-Iraqia University for supporting this research project.

■ CONFLICT OF INTEREST

There is no conflict of interest to declare.

■ AUTHOR CONTRIBUTIONS

Ahmed Mohammed Sulaiman led the research process and performed the final review of the manuscript. Abdulaziz Khaled Awwad prepared the complexes, conducted the spectroscopic measurements, and carried out the physical applications on the compounds. Both authors participated in writing the manuscript and in the analysis and interpretation of the results. All authors reviewed and agreed to the final version of this manuscript.

■ REFERENCES

[1] Rieth, A.J., Wright, A.M., and Dincă, M., 2019, Kinetic stability of metal–organic frameworks for corrosive and coordinating gas capture, *Nat. Rev. Mater.*, 4 (11), 708–725.

[2] Biswas, N., Datta, A., Manna, N.K., Mandal, D.K., and Gorla, R.S.R., 2021, Thermo-bioconvection of oxytactic microorganisms in porous media in the presence of magnetic field, *Int. J. Numer. Methods Heat Fluid Flow*, 31 (5), 1638–1661.

[3] Mey, A.S.J.S., Allen, B.K., Bruce Macdonald, H.E., Chodera, J.D., Hahn, D.F., Kuhn, M., Michel, J., Mobley, D.L., Naden, L.N., Prasad, S., Rizzi, A., Scheen, J., Shirts, M.R., Tresadern, G., and Xu, H., 2020, Best Practices for alchemical free energy calculations [Article v1.0], *Living J. Comput. Mol. Sci.*, 2 (1), 18378.

[4] Kettle, S.F.A., 1996, *Physical Inorganic Chemistry*, Springer Berlin, Heidelberg, Germany.

[5] Elsherif, K.M., Zubi, A., Najar, A., and Bin Ghashir, H., 2022, Determination of stoichiometry and stability constant of Cd(II) and Zn(II) complexes with pyrazole based ligands in mixed solvent (EtOH-H_2O), *J. Pure Appl. Sci.*, 21 (2), 128–134.

[6] Weber, B., 2023, "Stability of Coordination Compounds" in *Coordination Chemistry: Basics and Current Trends*, Springer Berlin, Heidelberg, Germany, 87–105.

[7] Gunatilake, S.K., 2015, Methods of removing heavy metals from industrial wastewater, *J. Multidicip. Eng. Sci. Stud.*, 1 (1), 12–18.

[8] Lewoyehu, M., 2021, Comprehensive review on synthesis and application of activated carbon from agricultural residues for the remediation of venomous pollutants in wastewater, *J. Anal. Appl. Pyrolysis*, 159, 105279.

[9] Ajiboye, T.O., Oyewo, O.A., and Onwudiwe, D.C., 2021, Simultaneous removal of organics and heavy metals from industrial wastewater: A review, *Chemosphere*, 262, 128379.

[10] Al-Khazraji, A.M.A., 2023, Synthesis of Co(II), Ni(II), Cu(II), Pd(II), and Pt(IV) complexes with $1^4,1^5,3^4,3^5$-tetrahydro-$1^1H,3^1H$-4,8-diaza-1,3(3,4)-ditriazola-2,6(1,4)-dibenzenacyclooctaphane-4,7-dien-15,35-dithione, and the thermal stability of polyvinyl chloride modified complexes, *Indones. J. Chem.*, 23 (3), 754–769.

[11] Perelonia, K.B.S., Benitez, K.C.D., Banicod, R.J.S., Tadifa, G.C., Cambia, F.D., and Montojo, U.M., 2021, Validation of an analytical method for the

determination of cadmium, lead and mercury in fish and fishery resources by graphite furnace and cold vapor atomic absorption spectrometry, *Food Control*, 130, 108363.

[12] Xu, Z., Zhang, Q., Li, X., and Huang, X., 2022, A critical review on chemical analysis of heavy metal complexes in water/wastewater and the mechanism of treatment methods, *Chem. Eng. J.*, 429, 131688.

[13] Ngah, F.A.A., Zakariah, E.I., Fakhar, I., Hassan, N.I., Heng, L.Y., Yamin, B., and Hasbullah, S.A., 2018, A new thiourea compound as potential ionophore for metal ion sensor, *Indones. J. Chem.*, 18 (1), 116–120.

[14] Zhang, T., Deng, G., Li, H., Liu, B., Tan, Q., and Xu, B., 2018, Cyclization of 2-biphenylthiols to dibenzothiophenes under $PdCl_2$/DMSO catalysis, *Org. Lett.*, 20 (17), 5439–5443.

[15] Enamullah, M., Uddin, A.K.M.R., Pescitelli, G., Berardozzi, R., Makhloufi, G., Vasylyeva, V., Chamayou, A.C., and Janiak, C., 2014, Induced chirality-at-metal and diastereoselectivity at Δ/Λ-configured distorted square-planar copper complexes by enantiopure Schiff base ligands: Combined circular dichroism, DFT and X-ray structural studies, *Dalton Trans.*, 43 (8), 3313–3329.

[16] Kilday, M.V., 1980, The enthalpy of solution of SRM 1655 (KCl) in H_2O, *J. Res. Natl. Bur. Stand.*, 85 (6), 467–482.

[17] Ono, T., Komatsu, Y., Sasaki, Y., Ota, M., Sato, Y., Takebayashi, Y., Furuya, T., and Inomata, H., 2022, Densities and viscosities of (ethylene glycol - water) and (1,3-propanediol - water) binary mixtures at high temperatures of 373.2 and 473.2 K and high pressures up to 40 MPa, *J. Mol. Liq.*, 349, 118096.

[18] Agarwal, S., Tyagi, I., Gupta, V.K., Ghasemi, N., Shahivand, M., and Ghasemi, M., 2016, Kinetics, equilibrium studies and thermodynamics of methylene blue adsorption on *Ephedra strobilacea* saw dust and modified using phosphoric acid and zinc chloride, *J. Mol. Liq.*, 218, 208–218.

[19] Fernandes, J.V., Rodrigues, A.M., Menezes, R.R., and Neves, G.A., 2020, Adsorption of anionic dye on the acid-functionalized bentonite, *Materials*, 13 (16), 3600.

[20] Phat, V.V., and Le Luu, T., 2023, Review on the removal of arsenic in groundwater using laterite adsorbent, *Curr. Opin. Environ. Sci. Health*, 35, 100496.

[21] Marouf, R., Dali, N., Boudouara, N., Ouadjenia, F., and Zahaf, F., 2021, "Study of Adsorption Properties of Bentonite Clay" in *Montmorillonite Clay*, Eds. Uddin, F., IntechOpen, Rijeka, Croatia.

[22] Mohammed, S.S., and Al-Heetimi, D.T.A., 2019, Adsorption of methyl violet dye from aqueous solution by Iraqi bentonite and surfactant – modified Iraqi bentonite, *Ibn Al-Haitham J. Pure Appl. Sci.*, 32 (3), 28–42.

[23] Gedik, E., and Atmaca, A., 2023, An experimental study investigating the effects of bentonite clay on mechanical and thermal properties of concrete, *Constr. Build. Mater.*, 383, 131279.

[24] dos Santos, R.M.M., Gonçalves, R.G.L., Constantino, V.R.L., Santilli, C.V., Borges, P.D., Tronto, J., and Pinto, F.G., 2017, Adsorption of Acid Yellow 42 dye on calcined layered double hydroxide: Effect of time, concentration, pH and temperature, *Appl. Clay Sci.*, 140, 132–139.

[25] Elsherif, K.M., Haider, I., and El-Hashani, A., 2019, Adsorption of Co(II) ions from aqueous solution onto tea and coffee powder: Equilibrium and kinetic studies, *J. Fundam. Appl. Sci.*, 11 (1), 65–81.

[26] Maderova, Z., Baldikova, E., Pospiskova, K., Safarik, I., and Safarikova, M., 2016, Removal of dyes by adsorption on magnetically modified activated sludge, *Int. J. Environ. Sci. Technol.*, 13 (7), 1653–1664.

[27] Huang, W.Y., Li, D., Liu, Z.Q., Tao, Q., Zhu, Y., Yang, J., and Zhang, Y.M., 2014, Kinetics, isotherm, thermodynamic, and adsorption mechanism studies of $La(OH)_3$-modified exfoliated vermiculites as highly efficient phosphate adsorbents, *Chem. Eng. J.*, 236, 191–201.

[28] Kindeel, A.S., Dawood, I.J., and Aziz, M.R., 2013, Synthesis and characterization of some mixed ligand complexes containing (8-hydroxyquinoline) and (2-picoline) with some metal ions, *Baghdad Sci. J.*, 10 (2), 14.

[29] Ayeleru, O.O., Modekwe, H.U., Onisuru, O.R., Ohoro, C.R., Akinnawo, C.A., and Olubambi, P.A., 2023, Adsorbent technologies and applications for carbon capture, and direct air capture in environmental perspective and sustainable climate action, *Sustainable Chem. Clim. Action*, 3, 100029.

[30] Hamzaoui, M., Bestani, B., and Benderdouche, N., 2018, The use of linear and nonlinear methods for adsorption isotherm optimization of basic green 4-dye onto sawdust-based activated carbon, *J. Mater. Environ. Sci.*, 9 (4), 1110–1118.

[31] Mekatel, E., Dahdouh, N., Samira, A., Nibou, D., and Trari, M., 2021, Removal of Maxilon Red dye by adsorption and photocatalysis: Optimum conditions, equilibrium, and kinetic studies, *Iran. J. Chem. Chem. Eng.*, 40 (1), 93–110.

[32] Rauf, N., Tahir, S.S., Kang, J.H., and Chang, Y.S., 2012, Equilibrium, thermodynamics and kinetics studies for the removal of alpha and beta endosulfan by adsorption onto bentonite clay, *Chem. Eng. J.*, 192, 369–376.